Ferrohydrodynamic Flow of Hybrid Magnetised Fluid with Magnetic Field-Dependent Viscosity over an Extending Plate

Nur Ilyana Kamis
Department of Mathematical Sciences, Faculty of Science, Universiti Teknologi Malaysia

Noraihan Afiqah Rawi
Department of Mathematical Sciences, Faculty of Science, Universiti Teknologi Malaysia

Lim Yeou Jiann
Department of Mathematical Sciences, Faculty of Science, Universiti Teknologi Malaysia

Sharidan Shafie
Department of Mathematical Sciences, Faculty of Science, Universiti Teknologi Malaysia

https://doi.org/10.5109/7395755

出版情報：Proceedings of International Exchange and Innovation Conference on Engineering & Sciences (IEICES). 11, pp.1845-1851, 2025-10-30. International Exchange and Innovation Conference on Engineering & Sciences
バージョン：

Ferrohydrodynamic Flow of Hybrid Magnetised Fluid with Magnetic Field-Dependent Viscosity over Extending Plate

Nur Ilyana Kamis, Noraihan Afiqah Rawi, Lim Yeou Jiann, Sharidan Shafie
Department of Mathematical Sciences, Faculty of Science, Universiti Teknologi Malaysia, 81310 Johor Bahru, Johor, Malaysia
Corresponding author email: noraihanafiqah@utm.my

Abstract: *Hybrid ferrofluid (HFF) contains magnetic nanoparticles that improve fluid flow and heat transfer, making them important for medical research. The study aims to investigate the behaviour of HFF flowing past an extending plate. The HFF is formed by combining ferrite and cobalt ferrite nanoparticles. Dispersing the HFF in a biopolymer solution of ethylene glycol (EG) mixed with water enhances its biocompatibility. The presence of a magnetic dipole as a source of magnetic fields introduces both magnetic field-dependent viscosity (MFDV) and ferrohydrodynamic (FHD) effects. The heat transfer problem is initially formulated using partial differential equations and then simplified into ordinary differential equations through a similarity transformation. These equations are solved using the Keller box method. The MFDV effect enhances fluid velocity but reduces the temperature profile. In contrast, the FHD effect decreases the velocity while increasing the fluid temperature. This study provides valuable insights for improving nanoparticle utilisation in biomedical applications.*

Keywords: Hybrid ferrofluid; MFDV; FHD; Keller box method

1. INTRODUCTION

Hybrid ferrofluid (HFF) is an advanced form of ferrofluid (FF) and a specialised type of hybrid nanofluid (HNF), known for its enhanced thermal and magnetic properties [1]. It consists of magnetic nanoparticles dispersed in a base fluid [2]. The inclusion of these magnetic nanoparticles imparts magnetic characteristics and significantly improves the fluid's thermal performance. This fluid has numerous potential applications in technical, industrial, and scientific fields, particularly in biomedical engineering, such as cancer treatment, magnetic resonance imaging (MRI), and targeted drug delivery [3-5]. For instance, the ability of magnetic nanoparticles to literally drag drug molecules to their target location when magnetic fields are applied makes them highly valuable for use as carriers of drugs, as shown in Fig. 1 [6]. The effectiveness of such magnetic nanoparticles has been further explored by Alam et al. [*insert ref*], who conducted a numerical analysis on nanofluid flow containing magnetic particles near a stretched cylinder in the presence of a magnetic dipole. Their findings underscore the potential of magnetic fields to enhance flow control and heat transfer, offering valuable insights for biomedical applications such as targeted therapy and thermal treatment. The other review on ferrite or magnetic nanoparticles can be found in the work reported by Protik *et al.* [8].

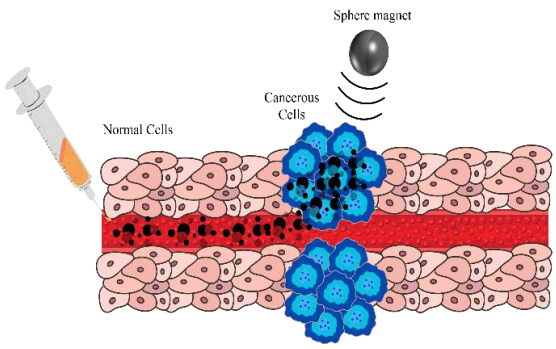

Fig.1 Targeted drug delivery system

It is important to note that Anderson and Valnes [9] were the first researchers to investigate the behaviour of FF flow over an extending plate. The FF flow is subjected to saturation under the influence of a magnetic dipole, which serves as the source of the magnetic field. The dipole is positioned at a certain distance beneath the flow and generates magnetic fields aligned with the flow direction, specifically in the positive $x-$direction. A magnetic dipole refers to a magnet or magnetic material with distinct north and south poles at opposite ends [10]. A compact spherical magnet generates stronger magnetic fields due to its closely spaced dipoles, resulting in a more intense magnetic field in its surrounding area. Neuringer and Rosensweig [11] stated that the application of magnetic fields to FF induces a response known as the ferrohydrodynamic (FHD) effect. This interaction between the FF and the magnetic field introduces additional complexities to the flow behaviour. Their findings revealed that the FHD effect decreases the velocity profile while increasing the thermal boundary layer thickness along the extending plate. As a result, FHD HFF flow over an extending plate has attracted considerable research interest due to its significant influence on velocity, temperature distributions, and related physical parameters.

Yang *et al.* [12] studied a HFF composed of ferrite (Fe_3O_4), manganese zinc ferrite ($MnZnFe_2O_4$) dispersed in both water and refrigerant-134A. They found that heat transfer in the HFF improves with increasing concentration of magnetic nanoparticles in the base fluid. Additionally, the temperature profile increased with higher viscous dissipation values [13], attributed to the heat generated by the FHD effect in the HFF. The velocity profile was observed to decrease more rapidly in the $MnZnFe_2O_4/Fe_3O_4$ hybrid compared to $MnZnFe_2O_4$ alone. Tahir *et al.* [14] further investigated the FHD behaviour of HFFs containing nickel zinc ferrite ($NiFe_2O_4$) and $MnZnFe_2O_4$ dispersed in kerosene and engine oil. The FHD effect in HFF flow has been extensively studied, as reported in recent research [15,16].

Additionally, the effect of magnetohydrodynamics (MHD) on HFF composed of Fe_3O_4 and cobalt ferrite ($CoFe_2O_4$) dispersed in water, without the influence of a magnetic dipole, has been studied by Idris *et al.* [2] and Zainodin *et al.* [17], and Nisar *et al.* [18].

The interaction between magnetic nanoparticles in a FF and an external magnetic field causes a significant change in the fluid's viscosity [19]. Viscosity, which measures a fluid's resistance to flow or deformation, reflects its "thickness" or "stickiness" [20]. Both theoretical and experimental studies have shown that magnetic fields influence the dynamic viscosity of fluids containing suspended magnetic nanoparticles [21, 22]. This behaviour is known as the magnetic field-dependent viscosity (MFDV) effect [23].

Khan *et al.* [24] investigated the MFDV effect in a FF flow over a squeezing, contracting disc. They defined the magnetic flux of the FF as the sum of magnetisation and magnetic field, following Rosensweig's formulation [25]. Their findings indicated that an increased MFDV effect leads to greater fluid resistance, thereby altering the velocity profiles near the disc surfaces. Furthermore, Khan *et al.* [26] extended the previous study by Khan *et al.* [24] by analysing the MFDV effect in FHD FF flow within rotating channels, incorporating viscous dissipation. Unlike the earlier study, they observed a decreasing trend in the Nusselt number. The results showed that the MFDV effect reduces the velocity near the bottom plate while increasing it near the upper plate. Shah *et al.* [27] studied the MFDV effect and radiative heat flux in FF flow over a rotating disc, considering suction and injection at the lower surface. Their findings showed a significant reduction in shear stress with increasing MFDV parameters. Similarly, Izadi *et al.* [22] analyzed the MFDV effect in micropolar nano-FF flow over a linear permeable extending plate. In a related study, Mehryan *et al.* [28] investigated a HFF composed of multi-walled carbon nanotubes (MWCNTs) and Fe_3O_4 nanoparticles suspended in water through a porous medium. They reported that the presence of the MFDV effect led to an increase in the Nusselt number.

Based on the reviewed literature, there is a noticeable lack of studies addressing the magnetic field-dependent viscosity (MFDV) effect in ferrofluid (FF) flows. Moreover, to the best of the authors' knowledge, no prior research has explored the influence of the MFDV effect on hybrid ferrofluid (HFF) flow in the presence of a magnetic dipole. Inspired by the findings of Izadi *et al.* [22], Shah *et al.* [27], and Mehryan *et al.* [28] the present study aims to address this gap by analysing the effect of MFDV on HFF flow. A magnetic dipole configuration, as described in [12, 13], is incorporated to account for the ferrohydrodynamic (FHD) influence.

The partial differential equations (PDEs) governing the FHD HFF flow with the MFDV effect are first established. These equations are then reduced to a system of ordinary differential equations (ODEs) using appropriate similarity transformations. Numerical solutions are obtained using the Keller box method in MATLAB. The analysis focuses on the effects of key physical parameters, evaluated through temperature and velocity profiles as well as critical engineering quantities. The main objectives of the present study are.

i. To investigate the effect of MFDV on the behaviour of FHD magnetised HFF.
ii. To examine the influence of ferrohydrodynamic (FHD) effects induced by a magnetic dipole on the magnetised HFF flow.

2. MATHEMATICAL FORMULATION

The present study considers steady, two-dimensional, incompressible, electrically non-conducting and laminar viscous hybrid ferrofluid (HFF) flow over an extending plate with a magnetic dipole in the presence of the magnetic field-dependent viscosity (MFDV) effect. The HFF is formed by dispersing ferrite and cobalt ferrite nanoparticles in a base fluid consisting of a 50%:50% mixture of ethylene glycol (EG) and water. The assumptions of the study are as follows.

i. The HFF flow is generated by the plate extending in the $x-$direction with a velocity $U_w = cx$, where c is a positive extending rate. The $y-$axis is taken as perpendicular to the plate [13].
ii. The plate surface is maintained at a constant temperature T_w , while T_∞ denotes the ambient temperature. The inclusion of magnetic nanoparticles introduces a characteristic temperature known as the Curie temperature T_c. The temperature of the HFF is represented by T. The temperature of the HFF is assumed to satisfy the condition $T < T_w < T_\infty < T_c$ [12].
iii. A magnetic dipole, positioned below the $x-$axis with its center aligned along the $y-$axis, generates the magnetic field. The vertical distance between the dipole and the sheet is denoted by d. The magnetic moment is directed along the positive $x-$axis (from the north to the south pole, as illustrated in Fig. 2), producing a magnetic field strong enough to saturate the HFF [13]. Since the HFF is electrically non-conducting, the magnetohydrodynamic (MHD) effect is neglected in this study. Thus, the mathematical modeling of the HFF is [13, 28]

$$\frac{\partial u}{\partial x} + \frac{\partial v}{\partial y} = 0, \tag{1}$$

$$\rho_{hff}\left(u\frac{\partial u}{\partial x} + v\frac{\partial u}{\partial y}\right) = M\mu_0\frac{\partial H}{\partial x} + \varrho_{hff}\left(\frac{\partial^2 u}{\partial x^2} + \frac{\partial^2 u}{\partial y^2}\right), \tag{2}$$

$$\left(\rho C_p\right)_{hff}\left(u\frac{\partial T}{\partial x} + v\frac{\partial T}{\partial y}\right) + \left(u\frac{\partial H}{\partial x} + v\frac{\partial H}{\partial y}\right)\mu_0 T\frac{\partial M}{\partial T} = k_{hff}\left(\frac{\partial^2 T}{\partial x^2} + \frac{\partial^2 T}{\partial y^2}\right) + \varrho_{hff}\left[2\left(\frac{\partial u}{\partial x}\right)^2 + 2\left(\frac{\partial v}{\partial y}\right)^2 + \left(\frac{\partial u}{\partial y} + \frac{\partial v}{\partial x}\right)^2\right]. \tag{3}$$

The governing PDEs (1) to (3) are subjected to the boundary conditions [9, 12, 13]

$$y = 0:\ u - U_w = 0, v = 0, T = T_w, \tag{4}$$

$$y \to \infty:\ u \to 0, T \to T_c. \tag{5}$$

Equation (1) represents the continuity equation, while Equation (2) corresponds to the Navier–Stokes momentum equation with the term $M\mu_0\frac{\partial H}{\partial x}$ represents the magnetic body force per unit volume [9]. The magnetization M in Equation (2) is assumed to vary

linearly with temperature and is defined as $M = K(T_c - T)$, where K is thermomagnetic effect [9]. The vector $\left\langle \frac{\partial H}{\partial x}, \frac{\partial H}{\partial y} \right\rangle$ represents the components of magnetic field gradient $\nabla \boldsymbol{H}$ which are derived from the magnetic scalar potential. Further details can be found in the work by Anderson and Valnes [9]. These components are given by $\frac{\partial H}{\partial x} = -\frac{\gamma_1}{2\pi} \frac{2x}{(y+d)^4}$, and $\frac{\partial H}{\partial y} = \frac{\gamma_1}{2\pi}\left(-\frac{2}{(y+d)^3} + \frac{4x^2}{(y+d)^5}\right)$ [9].

The term ϱ_{hff} appears in both Equations (2) and (3) to account for the MFDV effect. This viscosity is defined as $\varrho_{hff} = \mu_{hff}(1 + \boldsymbol{\delta} \cdot \boldsymbol{B})$, where μ_{hff} denotes the dynamic viscosity of the HFF, modelled based on the Tiwari and Das approach [28, 29]. The viscosity variation coefficient δ is assumed to be isotropic, such that $\delta_x = \delta_y = \delta$ [24, 26, 28]. The magnetic flux density (or magnetic induction) B is determined by the relationship $B = \mu_0(M + H)$ where M is the magnetisation, H is the applied magnetic field, and μ_0 is the magnetic permeability of free space [24, 26, 28]. For simplicity, a linear approximation is used in which $B = \mu_0(M_0 + H_0)$, representing constant magnetisation and magnetic field values [24, 26, 28]. Thus, the MFDV effect in the HFF flow is finally expressed as $\varrho_{hff} = \mu_{hff}[1 + \delta\mu_0(M_0 + H_0)]$ [24, 26, 28].

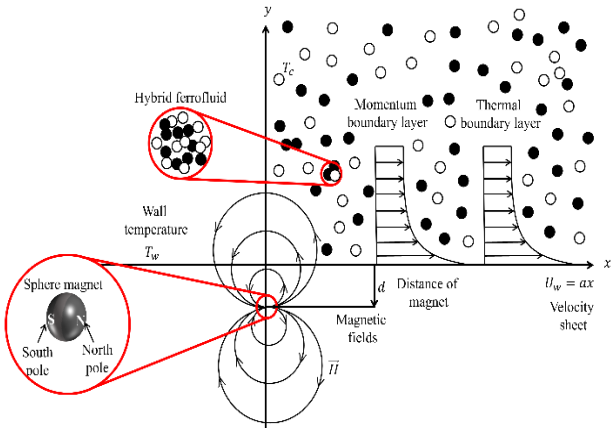

Fig. 2 Physical geometry

The complex PDEs (1) to (3) and boundary conditions (4) and (5) are simplified into ODEs using similarity transformations with the variables given below [13]

$$\psi(\xi,\eta) = \nu_f \xi f(\eta),$$
$$(\xi,\eta) = \left(\left(\frac{c}{\nu_f}\right)^{\frac{1}{2}} x, \left(\frac{c}{\nu_f}\right)^{\frac{1}{2}} y\right) \quad (6)$$
$$\theta(\xi,\eta) = \frac{T_c - T}{T_c - T_w} = \theta_1(\eta) + \xi^2\theta_2(\eta).$$

Here, $f(\eta)$ is the similarity function, and $\nu_f = \frac{\mu}{\rho}$ denotes the kinematic viscosity. The dimensionless temperature is represented by $\theta(\xi,\eta)$, while the stream function is denoted by $\psi(\xi,\eta)$, both depending on the variables (ξ,η). Notably, the stream function $\psi(\xi,\eta)$ satisfies the continuity equation (1). The velocity components of the HFF flow in the $x-$ and $y-$directions are given by $(u,v) = \left(-\left(c\nu_f^{-1}\right)^{0.5} f(\eta), cxf'(\eta)\right)$.

Substituting Equation (6) into the governing PDEs (2) and (3) yields the following reduced form.

$$\delta_{mf} f''' - \left(\frac{\rho_{hff}}{\rho_{cf}}\right)\left(\frac{\mu_{cf}}{\mu_{hff}}\right)[(-f'^2 + ff'')] - 2\left(\frac{\mu_{cf}}{\mu_{hff}}\right)\frac{\beta\theta_1}{(\eta+\alpha)^4} = 0, \quad (7)$$

$$\left(\frac{k_{hff}}{k_{cf}}\right)(\theta_1'' + 2\theta_2) + \left(\frac{(\rho C_p)_{hff}}{(\rho C_p)_{cf}}\right) Prf\theta_1' + \frac{2\chi\beta f(\theta_1 - \varepsilon)}{(\eta+\alpha)^3} - \left(\frac{\mu_{hff}}{\mu_{cf}}\right) 4\delta_{mf}\chi f'^2 = 0, \quad (8)$$

$$\left(\frac{k_{hff}}{k_{cf}}\right)\theta_2'' - \left(\frac{(\rho C_p)_{hff}}{(\rho C_p)_{cf}}\right) Pr(2f'\theta_2 - f\theta_2') + \frac{2\chi\beta f\theta_2}{(\eta+\alpha)^3} - \left(\frac{\mu_{hff}}{\mu_{cf}}\right)\chi\delta_{mf} f''^2 - \lambda\beta(\theta_1 - \varepsilon)\left[\frac{2f'}{(\eta+\alpha)^4} + \frac{4f}{(\eta+\alpha)^5}\right] = 0. \quad (9)$$

$$\text{at } \eta = 0: f(\eta) = 0, f'(\eta) = 1, \theta_1(\eta) = 1, \theta_2(\eta) = 0, \quad (10)$$

$$\text{at } \eta \to \infty: f'(\eta) \to 0, \theta_1(\eta) \to 0, \theta_2(\eta) \to 0. \quad (11)$$

The non-dimensional parameters are Prandtl number, $Pr = \frac{\mu C_\rho}{k}$, Curie temperature, $\varepsilon = \frac{T_c}{T_c - T_w}$, viscous dissipation, $\chi = \frac{c\mu^2}{\rho k(T_c - T_w)}$, dimensionless distance, $\alpha = \sqrt{\frac{c\rho}{\mu}}d$, FHD effect, $\beta = \frac{\gamma}{2\pi}\frac{\mu_0 K(T_c - T_w)\rho}{\mu^2}$ and MFDV effect,

$\delta_{mf} = 1 + \delta\mu_0(M_0 + H_0)$.

The dimensionless expressions for skin friction, C_f and Nusselt number, Nu_x with respect to the Reynolds number, $Re = U_w\left(\frac{x}{\nu_f}\right)$, are [12]

$$C_f Re_x^{\frac{1}{2}} = -\frac{2}{\mu_{hff}} f''(0) \text{ and}$$
$$Nu_x Re_x^{-\frac{1}{2}} = -\frac{k_{hff}}{k_{cf}}[\theta_1'(0) + \xi^2\theta_2'(0)].$$

The constant values of ferrite nanoparticles and base fluid can be seen in Table 1 [17, 18]

Table 1. The thermophysical traits of HFF

Properties	Fe_3O_4	$CoFe_2O_4$	EG with water (50%:50%)
$\rho(kgm^{-3})$	5180	4907	1056
$C_p(Jkg^{-1}K^{-1})$	670	700	3.288
$k(Wm^{-1}K^{-1})$	9.7	3.7	0.425
$\beta \times 10^{-5}(K^{-1})$	0.5	1.3	0.00341
Pr	-	-	29.86

$\rho_{hff}, (\rho C_p)_{hff}, (\rho\beta^*)_{hff}, \mu_{hff}$ and k_{hff} are density, specific heat capacity, thermal expansion coefficient, and thermal conductivity, respectively. These thermophysical properties with nanoparticles' concentration of ϕ are defined below [13]

$$\rho_{hff} = (1 - \phi_{CoFe_2O_4})$$

$$\left[(1-\phi_{Fe_3O_4})\rho_{EG+water}+\phi_{Fe_3O_4}\rho_{Fe_3O_4}\right]+\phi_{CoFe_2O_4}\rho_{CoFe_2O_4},$$

$$(\rho C_p)_{hff}=(1-\phi_{CoFe_2O_4})\left[\begin{matrix}(1-\phi_{Fe_3O_4})(\rho C_p)_{EG+water}+\\ \phi_{Fe_3O_4}(\rho C_p)_{Fe_3O_4}\end{matrix}\right]+\phi_{CoFe_2O_4}(\rho C_p)_{CoFe_2O_4},$$

$$(\rho\beta^*)_{hff}=(1-\phi_{CoFe_2O_4})\left[\begin{matrix}(1-\phi_{Fe_3O_4})(\rho\beta^*)_{EG+water}+\\ \phi_{Fe_3O_4}(\rho\beta^*)_{Fe_3O_4}\end{matrix}\right]+\phi_{CoFe_2O_4}(\rho\beta^*)_{CoFe_2O_4},$$

$$\mu_{hff}=\frac{\mu_{EG+water}}{(1-\phi_{Fe_3O_4})^{2.5}(1-\phi_{CoFe_2O_4})^{2.5}},$$

$$\frac{k_{hff}}{k_{Fe_3O_4}}=\frac{k_{CoFe_2O_4}+2k_{Fe_3O_4}-2\phi_{CoFe_2O_4}\left(k_{Fe_3O_4}-k_{CoFe_2O_4}\right)}{k_{CoFe_2O_4}+2k_{Fe_3O_4}+\phi_{CoFe_2O_4}\left(k_{Fe_3O_4}-k_{CoFe_2O_4}\right)}$$

where

$$\frac{k_{Fe_3O_4}}{k_{EG+water}}=\frac{k_{Fe_3O_4}+2k_{EG+water}-2\phi_{CoFe_2O_4}\left(k_{EG+water}-k_{Fe_3O_4}\right)}{k_{Fe_3O_4}+2k_{EG+water}+\phi_{CoFe_2O_4}\left(k_{EG+water}-k_{Fe_3O_4}\right)}$$

3. NUMERICAL METHOD

The system of ODEs is solved using the Keller box method, a well-established technique for solving nonlinear parabolic problems. This method is known for its unconditional stability and second-order accuracy [30]. The main steps are as follows:

i. The governing higher-order equations are rewritten as a system of first-order differential equations.
ii. The domain is divided into uniform grid points, and central difference approximations are applied at each midpoint.
iii. The equations are converted into finite difference form using the box scheme, which improves accuracy and stability.
iv. Nonlinear terms are linearised using Newton's method to allow for iterative solutions.
v. The resulting linear algebraic system is solved using the block tridiagonal elimination method at each iteration step.
vi. The process is repeated until the solution converges within a specified tolerance.

The Keller box method is implemented using MATLAB to carry out the numerical computations. Further details on the Keller box method can be found in references [31, 32].

4. RESULTS AND DISCUSSION

Table 2 demonstrates the comparison with studies reported by Khan and Pop [33] and Chouban and Chaudhary [13]. Both [13, 33] studied the FHD effect on the FF flow. The numerical results for $-\theta_1'(0)$ demonstrates good agreement with the published results. This has increased the reliability of the current study.

Table 2. Comparison of $-\theta_1'(0)$ for parameter of Pr when $\delta_{mf}=1$ and $\beta=\alpha=\varepsilon=\phi_1=\phi_2=0$

Pr	Khan and Pop [33]	Chouban and Chaudhary [13]	Present study
0.70	0.4539	0.4540	0.4538
2.00	0.9113	0.9113	0.9112
3.00	-	1.1653	1.1651
7.00	1.8954	1.8954	1.8953
10.0	-	2.3080	2.3079
20.0	3.3539	3.3539	3.3539
70.0	6.4621	6.4622	6.4622

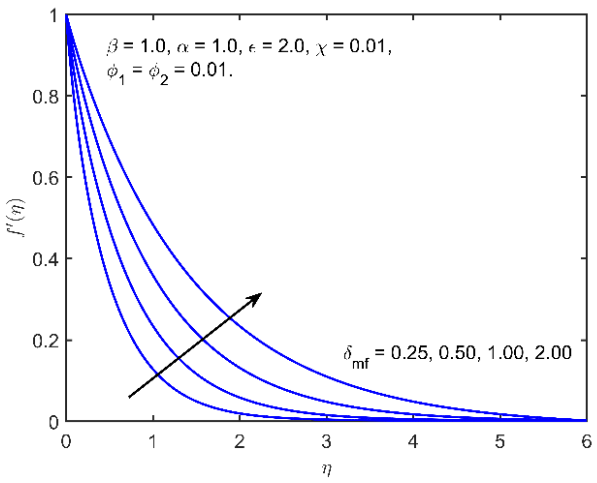

Fig. 3. MFDV effect over $f'(\eta)$

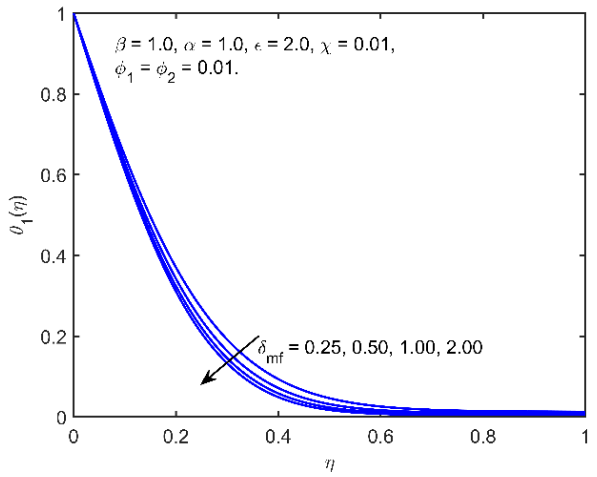

Fig. 4. MFDV effect over $\theta_1(\eta)$

The MFDV effect of parameter δ_{mf}, arises due to the interaction of the HFF with the magnetic fields generated by the magnetic dipole. Fig. 3 presents the effect of the parameter δ_{mf} on the profile of $f'(\eta)$ of the HFF. The increment of the parameter δ_{mf} from 0.25 to 2.00 reduces the viscosity of the HFF. The reduction in viscosity results in an increased $f'(\eta)$, allowing the HFF to move more freely and enhancing the thickness of the momentum boundary layer. The behaviour of $f'(\eta)$ aligns with the findings of Izadi *et al.* [22], which investigated the MFDV effect in FF flow. The current study shows that the MFDV effect has increased the profile of $f'(\eta)$ for the HFF flow.

A variational change in $\theta_1(\eta)$ due to the parameter δ_{mf} is plotted in Fig. 4. When the parameter δ_{mf} is elevated, then the profile of $\theta_1(\eta)$ is reduced. When the profile of $f'(\eta)$ increases, it enhances convection within the fluid while reducing conduction between the fluid and the wall of the sheet. As a result, the fluid temperature reduces and causing the thermal boundary layer to decrease near the sheet.

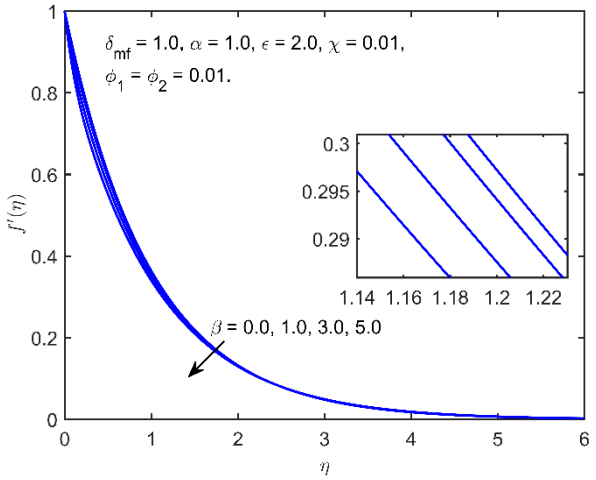

Fig. 5. FHD effect over $f'(\eta)$

The interaction between HFF and magnetic fields leads to the FHD effect presented by parameter β. The profile of $f'(\eta)$ under the effect of parameter β is depicted in Fig. 5. The FHD effect is enhanced as the values of parameter β expand from 0.0 to 5.0. The graph reveals that an increase in the parameter β leads to a reduction in the profile of $f'(\eta)$. The magnetic field induced by the magnetic dipole interacts with the HFF. This causes the saturation of the fluid and tends to escalate the development of magnetic chains or clusters. These chains or clusters change the viscosity of the fluid, which raises the effective viscosity of the HFF, thus, the fluid encounters more flow resistance. As a result, the movement of the HFF and momentum boundary layer thickness are reduced.

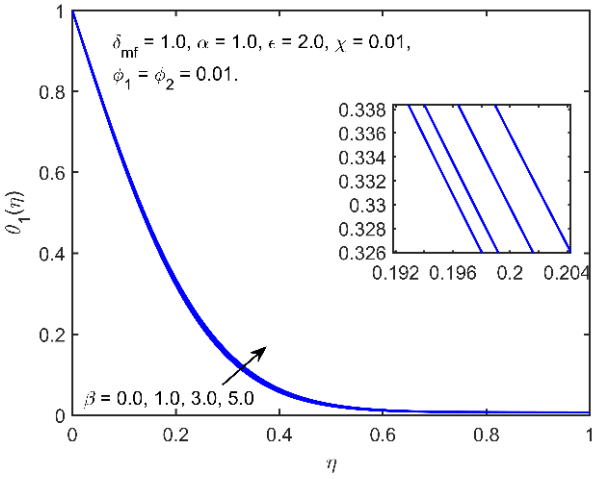

Fig. 6. FHD effect over $\theta_1(\eta)$

The FHD effect positively influences the temperature profile of $\theta_1(\eta)$, as seen in Fig. 6. As the fluid flows slowly, greater heat transfer occurs from the sheet to the fluid. Consequently, the temperature profile of $\theta_1(\eta)$ and the thermal boundary layer thickness increases. These findings align with the conclusions presented by Chouban and Chaudhary [13] who examined the FHD effect in the HFF flow.

Table 3. The values of $-C_f Re_x^{\frac{1}{2}}$ and $-Nu_x Re_x^{-\frac{1}{2}}$ for various δ_{mf}

δ_{mf}	$-C_f Re_x^{\frac{1}{2}}$	$-Nu_x Re_x^{-\frac{1}{2}}$
0.25	2.7100	3.3718
0.50	1.7831	3.6573
1.00	1.1922	3.8477
2.00	0.8089	3.9829

Table 3 presents the numerical results for the values of $C_f Re_x^{\frac{1}{2}}$, as the parameter δ_{mf} increases. The values of $C_f Re_x^{\frac{1}{2}}$ decrease with increasing parameter δ_{mf}. The parameter δ_{mf} reduces the viscosity of the fluid, which decreases the shear stress at the wall.

The change in the behaviour of $Nu_x Re_x^{-\frac{1}{2}}$ due to the parameter δ_{mf} increases is displayed in Table 5. It can be seen that the enhancement of the parameter δ_{mf} increases the values of $Nu_x Re_x^{-\frac{1}{2}}$. The increased $f'(\eta)$ indicates more vigorous fluid flow. This enhances convection within the fluid, while conduction between the wall and the fluid is reduced. These behaviours of $C_f Re_x^{\frac{1}{2}}$and $Nu_x Re_x^{-\frac{1}{2}}$ for the HFF aligns with the findings on the MFDV effect on HFF flow reported by Khan *et al.* [24] and Shah *et al.* [27].

5. CONCLUSION

This study explores the influence of magnetic field-dependent viscosity (MFDV) arising from the interaction between ferrohydrodynamic (FHD) effects and ferrite-based nanoparticles within hybrid ferrofluid (HFF) flow over an extending plate. The HFF is composed of magnetised nanoparticles, specifically ferrite (Fe_3O_4) and cobalt ferrite ($CoFe_2O_4$) dispersed in a biopolymer-based fluid consisting of ethylene glycol (EG) mixed with water. The governing equations are solved using the Keller box method implemented in MATLAB. A comprehensive investigation and discussion of the relevant parameters are presented, highlighting significant findings such as

i. both the velocity and temperature distributions of the HFF increase as the MFDV effect increases,
ii. the MFDV parameter has a stronger effect on the velocity field than on the temperature field,
iii. the velocity profile decreases, while the temperature profile increases as a result of the FHD effect.

The presence of MFDV and FHD effects plays a crucial role in optimising the efficiency of cancer therapy. Controlling the MFDV effect during treatment is essential to ensure effective drug accumulation at the cancer site. A magnetic dipole can direct drug-coated HFF toward the targeted area by influencing its motion in response to the magnetic field. The current findings offer valuable insights into optimising nanoparticle use within the HFF to maintain a therapeutic temperature.

In this study, the HFF is modelled as a Newtonian fluid. However, many real-world fluids, such as blood, polymer-based solutions, and nanofluid used in drug

delivery, exhibit non-Newtonian behaviour, meaning their viscosity varies with shear rate. Future studies could explore hybrid ferrofluid flow using non-Newtonian models, such as Casson fluid [34], which accounts for yield stress effects and is often applied in blood flow studies.

6. REFERENCES

[1] M. Kole, S. Khandekar, Engineering applications of ferrofluids: A review, J. Magn. Magn. Mater. 537 (2021) 168222.

[2] S. Idris, A. Jamaludin, R. Nazar, I. Pop, Heat transfer characteristics of magnetized hybrid ferrofluid flow over a permeable moving surface with viscous dissipation effect, Heliyon 9 (2023).

[3] J. Philip, P. Shima, B. Raj, Enhancement of thermal conductivity in magnetite based nanofluid due to chainlike structures, Appl. Phys. Lett. 91 (2007).

[4] M. Krichler, S. Odenbach, Thermal conductivity measurements on ferrofluids with special reference to measuring arrangement, J. Magn. Magn. Mater. 326 (2013) 85–90.

[5] N. Neogi, K.P. Choudhury, Utilization of metal based nanoparticles in biomedical imaging technologies, Chem. Biol. Lett. 10 (2023).

[6] Y.P. Yew, N.S. Shameli, M. Miyake, A. Ahmad, Green biosynthesis of superparamagnetic magnetite Fe_3O_4 nanoparticles and biomedical applications in targeted anticancer drug delivery system: A review, Arab. J. Chem. 13 (2020) 2287–2308.

[7] J. Alam, M.G. Murtaza, E.E. Tzirtzilakis, M. Ferdows, Mixed convection flow and heat transfer of Biomagnetic fluid with magnetic/non-magnetic particles due to a stretched cylinder in the presence of a magnetic dipole, Proc. Int. Exch. Innov. Conf. Eng. Sci. 8 (2022) 76–83.

[8] T.I. Protik, K.P. Choudhury, N. Neogi, S. Hossain, A.I. Helal, M.G. Sazid, An overview and statistical study on photocatalytic activities of Fe-based metal oxide nanoparticles, Nano Res. Appl. 9 (2023).

[9] H. Andersson, O. Valnes, Flow of a heated ferrofluid over a stretching sheet in the presence of a magnetic dipole, Acta Mech. 128 (1998) 39–47.

[10] K. Seleznyova, M. Strugatsky, J. Kliava, Modelling the magnetic dipole, Eur. J. Phys. 37 (2016).

[11] J.L. Neuringer, R.E. Rosensweig, Ferrohydrodynamics, Phys. Fluids 7 (1964) 1927–1937.

[12] J. Yang, Z. Abdelmalek, N. Muhammad, M. Mustafa, Hydrodynamics and ferrite nanoparticles in hybrid nanofluid, Int. Commun. Heat Mass Transf. 118 (2020).

[13] K.K. Chouhan, S. Chaudhary, Hybrid ferrofluid flow on a stretching sheet with Stefan blowing and magnetic polarization effects in a porous medium, Multidiscip. Model. Mater. Struct. (2024).

[14] H. Tahir, U. Khan, A. Din, Y.-M. Chu, N. Muhammad, X.-M. Li, Hybridized two phase ferromagnetic nanofluid with $NiZnFe_2O_4$ and $MnZnFe_2O_4$, Ain Shams Eng. J. 12 (2021) 3063–3070.

[15] N.I. Kamis, L.Y. Jiann, S. Shafie, N.A. Rawi, Magnetoviscous effects in magnetized dual-ferrofluid flow over an extending slippery plate, Arab. J. Sci. Eng. (2025).

[16] N.I. Kamis, L.Y. Jiann, N.A. Rawi, S. Shafie, Mixed convection of ferrohydrodynamics magnetized hybrid ferrofluid on a slip-permeable stretching sheet, J. Taibah Univ. Sci. 18 (2024).

[17] S. Zainodin, A. Jamaludin, R. Nazar, I. Pop, MHD mixed convection of hybrid ferrofluid flow over an exponentially stretching/shrinking surface with heat source/sink and velocity slip, Mathematics 10 (2022) 4400.

[18] K.S. Nisar, U. Khan, A. Zaib, I. Khan, D. Baleanu, Numerical simulation of mixed convection squeezing flow of a hybrid nanofluid containing magnetized ferroparticles in 50%:50% of ethylene glycol–water mixture base fluids between two disks with the presence of a non-linear thermal radiation heat flux, Front. Chem. 8 (2020) 792.

[19] E. Esmaeilnezhad, H.J. Choi, M. Schaffie, M. Gholizadeh, M. Ranjbar, S.H. Kwon, Rheological analysis of magnetite added carbonyl iron based magnetorheological fluid, J. Magn. Magn. Mater. 444 (2017) 161–167.

[20] F.M. White, J. Majdalani, Viscous Fluid Flow, McGraw-Hill, New York, 2006.

[21] Sunil, A. Sharma, D. Sharma, P. Kumar, Effect of magnetic field–dependent viscosity on thermal convection in a ferromagnetic fluid, Chem. Eng. Commun. 195 (2008) 571–583.

[22] M. Izadi, M. Javanahram, S.M.H. Zadeh, D. Jing, Hydrodynamic and heat transfer properties of magnetic fluid in porous medium considering nanoparticle shapes and magnetic field-dependent viscosity, Chin. J. Chem. Eng. 28 (2020) 329–339.

[23] S. Odenbach, S. Thurm, Magnetoviscous effects in ferrofluids, in: S. Odenbach (Ed.), Ferrofluids: Magnetically Controllable Fluids and Their Applications, Springer, Berlin, 2002, pp. 185–201.

[24] A. Khan, R.A. Shah, M. Shuaib, A. Ali, Fluid dynamics of the magnetic field dependent thermosolutal convection and viscosity between coaxial contracting discs, Results Phys. 9 (2018) 923–938.

[25] R. Rosensweig, Directions in ferrohydrodynamics, J. Appl. Phys. 57 (1985) 4259–4264.

[26] A. Khan, M. Yaqoob, H. Gul, M. Shuaib, A. Ali, Hydrodynamic analysis of the magnetic field dependent viscous fluid flow and thermosolutal convection between rotating channels, Sci. Rep. 12 (2022) 17170.

[27] R.A. Shah, A. Khan, A. Ali, Parametric analysis of magnetic field-dependent viscosity and advection–diffusion between rotating discs, Adv. Compos. Lett. 29 (2020).

[28] S. Mehryan, M. Izadi, Z. Namazian, A.J. Chamkha, Natural convection of multi-walled carbon nanotube–Fe_3O_4/water magnetic hybrid nanofluid flowing in porous medium considering the impacts of magnetic field-dependent viscosity, J. Therm. Anal. Calorim. 138 (2019) 1541–1555.

[29] R.K. Tiwari, M.K. Das, Heat transfer augmentation in a two-sided lid-driven differentially heated square cavity utilizing nanofluids, Int. J. Heat Mass Transf. 50 (2007) 2002–2018.

[30] I. Ullah, I. Khan, S. Shafie, Heat and mass transfer in unsteady MHD slip flow of Casson fluid over a moving wedge embedded in a porous medium in the

presence of chemical reaction: Numerical Solutions using Keller-Box Method, Numer. Methods Partial Differ. Equ. 34 (2018) 1867–1891.
[31] T. Cebeci, P. Bradshaw, Physical and Computational Aspects of Convective Heat Transfer, Springer, New York, 1988.
[32] N.I. Kamis, L.Y. Jiann, S. Shafie, N.A. Rawi, Comparative analysis of $Fe_3O_4/CoFe_2O_4$ and $NiZnFe_2O_4/MnZnFe_2O_4$ hybrid ferro-nanofluids flow under magnetic dipole effect over a slip stretching sheet, Case Stud. Therm. Eng. 51 (2023).
[33] W.A. Khan, I. Pop, Boundary-layer flow of a nanofluid past a stretching sheet, Int. J. Heat Mass Transf. 53 (2010) 2477–2483.
[34] N.I. Kamis, M.F.M. Basir, S. Shafie, T.K.A. Khairuddin, L.Y. Jiann, Suction effect on an unsteady Casson hybrid nanofluid film past a stretching sheet with heat transfer analysis, IOP Conf. Ser. Mater. Sci. Eng. 1078 (2021).